Sensitization of ON bipolar cells with ambient light activatable Multi-characteristic opsin rescues vision in mice

Subrata Batabyal, **Sivakumar Gajjeraman**, **Sanjay Pradhan**, **Sulagna Bhattacharya**, **Weldon Wright**, **Samarendra Mohanty**[*]

Nanoscope Technologies LLC, Bedford, TX 76022, USA.

Abstract

Gene therapy-based treatment such as optogenetics offers a potentially powerful way to bypass damaged photoreceptors in retinal degenerative diseases and use the remaining retinal cells for functionalization to achieve photosensitivity. However, current approaches of optogenetic treatment rely on opsins that require high intensity light for activation thus adding to the challenge for use as part of a wearable device. Here, we report AAV2 assisted delivery of highly photosensitive multi-characteristic opsin (MCO1) into ON bipolar cells of mice with retinal degeneration to allow activation by ambient light. Rigorous characterization of delivery efficacy by different doses of AAV2 carrying MCO1 (vMCO1) into targeted cells showed durable expression over 6 months after delivery as measured by reporter expression. The enduring MCO1 expression was correlated with the significantly improved behavioral outcome, that was longitudinally measured by visual water maze and optomotor assays. The pro/anti-inflammatory cytokine levels in plasma and vitreous humor of the vMCO1 injected group did not change significantly from baseline or control group. Furthermore, biodistribution studies at various time points after injection in animal groups injected with different doses of vMCO1 showed non-detectable vector copies in non-targeted tissues. Immunohistochemistry of vMCO1 transfected retinal tissues showed bipolar specific expression of MCO1 and the absence of immune/inflammatory response. Furthermore, ocular imaging using SDOCT showed no change in the structural architecture of vMCO1-injected eyes. Induction of ambient light-responsiveness to remaining healthy bipolar cells in subjects with retinal degeneration will allow the retinal circuitry to gain visual acuity without requiring an active stimulation device.

Introduction

Severe loss of vision occurs(1) due to Retinitis Pigmentosa (RP) and age-related macular degeneration (AMD) and approximately 11 million people in the US have some form of retinal degeneration, which is expected to double by 2050. RP and the dry form of macular degeneration(2-4) (dry-AMD), in which photoreceptors degenerate and are unable to produce the signals that initiate visual perception, account for 90 percent of the diagnosed cases. Retinal prostheses offer the possibility of restoring limited vision (5). Current systems, however, are limited by poor resolution (6, 7), retinal damage due to prolonged use, and the risk of inflammation and scar formation leading to chronic consequences (8, 9). Most of the current clinical treatments are primarily focused on slowing down the progression of the disease, as there is neither a cure that can stop the degeneration(10) nor a therapy, other than retinal prostheses (11), that can restore vision loss due to the retinal degeneration (12). Though retinal prostheses have been successful in generating limited visual perception in blind subjects (13-18), they have several limitations, such as cellular outgrowth, chronic damage of the implanted electrodes, and insufficient (sub-retinal) or disordered (epi-retinal) stimulation of retina (19, 20).

Genetically and chemically engineered light-gated ionotropic glutamate receptor(21, 22) or synthetic small molecule photo-switch (23), have been shown to photosensitize RGCs, leading to improved visually-guided behavior. Optogenetic sensitization (24-29) of retinal cells combined with activation/inhibition, has potential as an alternative to retinal implants. Expression of opsin allows for the flow of specific ions by light-induced trans-cis isomerization of all-trans-retinal, and thus, depolarizing/hyper-polarizing the opsin-expressing retinal cells when illuminated by the light of the characteristic wavelength of the opsin. This has allowed the possibility of replacing the retinal implants and eliminating the need to increase the number of electrodes for higher resolution. By bypassing the dysfunctional photoreceptors and engineering light-responsiveness in remaining healthy retinal cells, optogenetic treatment re-establishes the lost function of the retinal circuitry, leading to visual perception in blind subjects (24, 30). In addition to higher resolution (determined by sensitized retinal cells: RGCs, Bipolar cells), optogenetic treatment has several advantages over electrical stimulation such as cellular specificity (e.g. residual cones, ganglion or bipolar cells) and not requiring complex intraocular surgery (27, 28, 31). Promoter-specific expression of opsin in ON or OFF retinal cells, and restoration of ON and OFF light responses at the RGC and visual cortex level has been achieved(32),(33). Further, it has been shown in monkeys that pharmacologically blocking the OFF pathway does not impair the visual acuity, while it may affect the sensitivity to detect light decrement (34). Therefore, optogenetic based vision therapy may not be limited by the OFF-response.

However, the successful clinical translation of optogenetics based gene therapy suffers from the drawback of overall lower amplification of the currently used opsin photo-actuators thus necessitating the use of either an active stimulation device or prosthetic goggle for boosting the available ambient light. Long term active stimulation with high intensity light poses the risk of retinal damage and adds complexity to the treatment. To circumvent the limitation of current optogenetics technology, we have engineered an ambient light (<10 $\mu W/mm^2$) sensitive opsin (MCO1) having high temporal precision and a lower threshold

required for optogenetic stimulation (24). Here, we demonstrate the use of AAV2 packaged MCO1 (vMCO1), to selectively transfect the upstream-located second order retinal cells (ON bipolar cells) that receive synaptic input from photoreceptor cells. Use of optogenetic sensitization of bipolar cells (selective transduction by mGluR6 promoter) over RGCs have several advantages as optogenetic actuators such as they: (i) are preserved in degenerative retinal diseases, (ii) are close to the photoreceptors as compared to RGCs, preserving as much as possible the visual processing circuitry, (iii) are larger in number as compared to RGCs, providing higher spatial resolution, and (iv) do not have lateral extending processes (unlike RGCs), providing focal activation. In this study, we have thoroughly evaluated the long-term efficacy and safety of vMCO1-sensitized degenerated-retina in a murine model (*rd10*).

Results

Expression of MCO1 in retinal explant of rd10 mice led to significant photocurrent

MCO1 with ON bipolar cell specific promoter (mGluR6) were designed and synthesized using a DNA synthesizer. The theoretical modeling predicts that MCO1-mCherry is structurally 46% alpha helices, 17% beta sheets, 36% of random coils and 1% disordered. For *in-vivo* intravitreal injection, MCO1-mCherry plasmid was packed in rAAV2 virus (vMCO1). To determine the titer of vMCO1, a quantitative PCR based assay was carried out. The PCR baseline subtracted curve fit data (Suppl. Fig. S1A) and protein components (Suppl. Fig. S1B) of vMCO1 are shown in Suppl. Fig. S1. The fluorescence image of retinal cells in an explant of *rd10* mouse 4 days after transfection of MCO1, using lipofection, is shown in Fig. 1A. The expression is confirmed by the red fluorescence signal from the reporter gene (mCherry). The retinal cell expressing MCO1 exposed to a train of white light pulses generated repeated inward photocurrents (Fig. 1B). Representative intensity dependent photocurrent profiles are shown in Fig. 1C, while Fig. 1D shows quantitative comparison of evoked peak current in response to different stimulation intensities.

In-vivo persistent transduction of MCO1-mCherry in rd10 mice retina peaked at 4 weeks

In-vivo transduction of vMCO1 in *rd10* mouse retina was carried out for three different doses of 1μl of vMCO1 (1.0×10^{13}, 1.0×10^{12} and 1.0×10^{11} vg/ml), which is 1.0×10^{10}, 1.0×10^{9} and 1.0×10^{8} vg/eye respectively. Absence of characteristic mCherry expression (only background autofluorescence) in the control PBS injected mice eyes were observed up to 16 weeks (Suppl. Fig. S2A & B). Further, no significant increase in mCherry expression was observed 1 week after injection (Fig. 2A, Suppl. Fig. S2C). Expression of the reporter gene was significantly higher at 4-8 weeks after intravitreal injection of vMCO1 (Fig. 2B). Fig. 2C shows a cross-sectional view of MCO1 expression in retina after 16 weeks of vMCO1 (1.0×10^{10} vg) intravitreal injection. MCO1-mCherry expression was found to be localized in inner nuclear layer and in synaptic terminals near ganglion cell layer. Fig. 2D shows kinetics of MCO1 expression in *rd10* mice retina at three different doses of vMCO1. MCO1 expression was found to peak around 4 weeks after injection, with expression remaining stable even 16 weeks after injection.

Intravitreal injection of vMCO1 in rd10 mice led to ambient-light guided locomotion in a longitudinal manner

To test spatial memory and learning capabilities of vMCO1 treated *rd10* mice towards light, visual radial arm water maze was utilized (35). Visually guided locomotion in this test was determined by measuring the latency to reach the platform as the quality of the visual stimulus (cue) degrades. The platform provides a reward as a place where they can rest instead of having to swim. To demonstrate the efficacy of intravitreal injection of vMCO1 in vision restoration, mice with advanced/complete loss of photosensitivity were selected by pre-screening (Suppl. Fig. 3) using a visual radial water maze (Fig. 3A). Pre-screening means selection of animals with complete photoreceptor degeneration, which cannot find the lighted platform within 60 sec (even if they were trained to find the lighted platform at a juvenile age). The phenotype of *rd10* mice was confirmed by OCT analysis of retinal thickness (Suppl. Fig. S3A, B) and fundoscopy (Suppl. Fig. S3C). Suppl. Fig. S3D shows the time to reach the platform (with white LED light directed towards center of maze) from center of the water maze as a function of age. The latency to reach the platform was found to increase with increasing age of the mice, indicating progressive retinal degeneration. 12 weeks after birth, the *rd10* mice (screened for complete photoreceptor degeneration) were intravitreally injected with vMCO1 targeted to bipolar cells in retina. We collected data to determine visually guided locomotion at baseline (pre-viral injection), and over time (every 4 weeks for 16 weeks). Figs. 3B-D show results of the longitudinal study on visually guided improvement in *rd10* mice locomotion from center (Fig. 3B), (near) arm (Fig. 3C), and side (Fig. 3D) of the radial water maze at light intensity level of 1-7 $\mu W/mm^2$. All mice showed a significant restoration of their visually guided behavior 4-8 weeks after vMCO1 injection that lasted through the 16 weeks trial with the light intensity in the ambient level ($<10 \mu W/mm^2$). The mean number of arms swam by the vMCO1 injected *rd10* mice before they reached the platform is significantly smaller (<1) than that of the mice without injection (>2).

In addition, a group of *rd10* mice were subjected to water maze behavior study having variable visual intensity stimulus ($L_0=0.5 \mu W/mm^2$; $L_2 = 7 \mu W/mm^2$) from the center of the platform. The latency to reach the platform was found to significantly increase in case of lower intensity ($L_0=0.5 \mu W/mm^2$) of visual cue as compared to the relatively higher light intensity ($L_2 = 7 \mu W/mm^2$) (Suppl. Fig. S4). For the control behavior study, a cohort of mice (n=3) was injected with carrier rAAV2. The visually guided behavior of the *rd10* mice with intravitreal vehicle injection (rAAV2, 1 μL/eye) showed no statistically significant changes in the latency to find platform (associated with light) before and after injection (Suppl. Fig. S5). Dose response of vMCO1 along with AAV2 vehicle control was measured by water maze latency score of mice from center (Fig. 3E) and side (Fig. 3F). The intraocular dose range of $1.0 \times 10^8 - 1.0 \times 10^{10}$ vg was found to be therapeutically effective. The statistical analysis of vMCO1dose dependent improvement in behavior of *rd10* in radial water maze assay, carried out by one-way ANOVA with Tukey post hoc analysis, is shown in Supplementary Table S1.

Improvement of optomotor response in vMCO1 treated rd10 mice at ambient light level

Measurement of the optomotor response, frequently used to determine thresholds of the visual acuity in animals (36, 37), (38), was utilized to evaluate the improvement of visual performance of *rd10* mice with vMCO1 sensitized retinas. Intravitreal injection of vMCO1 into *rd10* mice increased the number of head movements (optomotor response) at different speeds of rotation of the vertical stripes (0.1 *cpd*). Quantitative comparison of number of head movement before and 8 weeks after intravitreal injection of vMCO1 at different speeds of rotation of the vertical stripes is shown in Fig. 4.

Our results show improved optomotor response in vMCO1 treated *rd10* mice at ambient light level (1 $\mu W/mm^2$). Improved visual acuity in addition to rescuing the phenotypic deficit in *rd10* mice, after transduction with the ambient-light activatable MCO1 into ON bipolar cells of retina, demonstrates the potential of MCO1 in vision restoration in subjects with retinal degenerative diseases.

No detectable increase in inflammatory response in plasma or vitreous humor after vMCO1 injection

Since gene therapy in humans has been controversial for the last decade due to undesired side effects (39, 40), we carried out immunotoxicity analysis of serum to quantify immune response after vMCO1 injection. *Rd10* mice serum was analyzed at different time points before and after vMCO1 administration. Studies on kinetics of immunotoxicity were conducted using mouse Picokine ELISA (BosterBio) based quantification of different pro (IL-6) and anti-inflammatory (IL-10) cytokines in the plasma of vMCO1-treated animals. Fig. 5 shows quantitative comparison of pro- and anti-inflammatory markers (IL6, IL-10) before and after 1 week to 6 weeks of vMCO1 injection in three different dose groups (group-1: 1.0×10^8 vg, group-2: 1.0×10^9 vg and group-3: 0.84×10^{10} vg). After 4 weeks of vMCO1 injection, there was no significant difference in the level of IL-6 and IL-10 in the serum as compared to the basal level (before injection).

In Fig. 6A, we show quantitative comparison of IL-6 in vitreous humor of *rd10* mice injected with vMCO1 (1.0×10^9 vg, in eye), 6 months after vMCO1 injection, and non-injected control. Similar to IL-6, no detectable change in IL-10 in vitreous humor of vMCO1-injected and non-injected control *rd10* mice groups was observed (Fig. 6B).

No detectable immune response in plasma of vMCO1 injected mice

The neutralizing antibody assay was performed to evaluate any pre-existing antibody for vMCO1 and to monitor the changes in the neutralizing antibody level following vMCO1 injection. The concentration of Neutralizing Antibody against vMCO1 was calculated by generating the standard curve (plotted using serial dilution of stock antibody solution). Fig. 6C shows longitudinal monitoring of the neutralizing Antibody (nAb) level in serum of *rd10* mice injected with vMCO1 (1.0×10^9 vg in eye) before and after injection. In Fig. 6D, we show the scatter plot of the mean and variation of measured neutralizing antibody concentration in serum of vMCO1 injected rd10 mice at each time point. Longitudinal monitoring of neutralizing antibody level in serum of *rd10* mice before and after vMCO1

injection (Fig. 6C) showed that there is no increase in the neutralizing antibody level after injection with vMCO1 (1.0×10^9 vg in eye) as compared to baseline values.

Pharmacokinetics and biodistribution studies show non-detectable levels of the vector in non-targeted organs of intravitreally-injected rd10 mice

To determine vector shedding and biodistribution of vMCO1 in non-targeted organs, following intravitreal injection of different doses of vMCO1, mice were serially sacrificed at various times up to 16 weeks following dosing for collection of tissue samples. Total DNA was extracted from the blood and major tissues (Brain, Eye, Heart, Kidney, Liver, and Spleen) and were analyzed using quantitative PCR to assess the level of AAV2 genomes. Fig. 7 shows the measured vector copy number (per ng of DNA) at different intravitreal vMCO1 injection doses at multiple time points. At a fixed time point after injection (1 week), the measured vector copy number in the eye was found to decrease with lowering of the injected vMCO1 dose. Furthermore, 4-8 weeks after injection, very small, or non-detectable quantities of vector DNA in the injected eyes were found. This may be attributed to the fact the left-over eye-tissues (after slicing of posterior part, i.e. retina) were used for biodistribution analysis by QPCR. Most non-eye tissues were negative for AAV2 genomes. There were sporadic, very low positive signals in the non-eye tissues (e.g. blood). Intravitreal administration of vMCO1 in eye is thus found to be locally-restricted distribution, minimizing off-target effects.

No detectable structural damage due to vMCO1 injection

Optical sectioning/imaging using SD-OCT was carried out to monitor any changes in ocular structure due to intravitreal injection of vMCO1 (N=4). Suppl. Fig. S6 A & B show SD-OCT images of *rd10* mice cornea, lens, and retina before vMCO1 injection. Suppl. Fig. S6C show SD-OCT images of *rd10* mice retina after vMCO1 injection. No detectable alteration to cornea, lens or retina (e.g. detachment) was observed due to intravitreal injection of vMCO1. Quantitative comparison of retinal thickness before and 1 week after injection shows no statistically significant differences (Suppl. Fig. S6D).

Intravitreal injection of vMCO1 led to ON-bipolar specific expression in retina without causing inflammatory-response

To confirm cell-specific expression of MCO-mCherry, vMCO1 injected *rd10* mice retina slices were immunostained for S-arrestin (photoreceptor), PKCα (bipolar cell) and mCherry (reporter for MCO1) and imaged with confocal microscopy 8 weeks after intravitreal injection. In Fig. 8A, PKCα staining (green) shows the expression of mCherry (intrinsic red fluorescence, Fig. 8B) is localized in rod bipolar cells. High levels of colocalization with virally expressed MCO1 in bipolar cells is evident in Fig. 8C. Zoomed imaging of the retinal section shows membrane expression of MCO1-mCherry in bipolar cells (Fig. 8Di) and co-localization of mCherry and PKCα (Fig. 8Dii). The absence of visual arrestin marker (Fig. 8E) in the mice retina revealed complete loss of photoreceptor layers.

To determine if any inflammatory response resulted from the intravitreal injection of vMCO1, the *rd10* mice retina slices were immunostained for CD45 (leukocyte common antigen) and glial fibrillary acidic protein (GFAP). Anti-CD45 staining was found to be

negative (Fig. 8G), confirming the absence of inflammatory cells in the retina 16 weeks after injection of vMCO1 (1.0 x 10^{10} vg/eye). The signature of GFAP was detected on the vitreal side of the retina in anti-GFAP staining (Fig. 8F), which is expected for photoreceptor degenerated mice(41). No increase in GFAP signal was observed in vMCO-1(3.5×10^9 vg/eye) injected mice eyes 6 months after bilateral injection as compared to non-injected control (Figs. 9A-B). Quantification of fluorescence intensity of GFAP-labeled retina for individual mice (F1-F5) showed no statistically significant difference in fluorescence intensity of GFAP-labeled retina between the vMCO1-injected group and negative control. To determine change in microglia response after vMCO1 injection, the cryo-sectioned retinal slices were immunostained for Iba1. Figs. 9E and F show the representative confocal fluorescence microscope image of Iba1-stained retina in non-injected control and vMCO1(3.5×10^9 vg/eye) injected mice eyes 6 months after bilateral injection. Quantification of Iba1+ve cells for individual mice showed inter-animal variability, however, no statistically significant difference in Iba1+ cells was found between the vMCO1-injected group and negative control.

Discussion

We demonstrated behavioral restoration of vision in mice models with retinal degeneration at ambient-light level (<10 $\mu W/mm^2$) upon sensitization of the retinal bipolar cells using intravitreal injection of vMCO1. Enhanced light sensitivity was seen in two visually guided behavioral assays: radial water maze and optomotor response. These behavioral outcomes correlate the MCO expression level. Our results demonstrated that the bipolar cell layers in the mice retina can be efficiently sensitized, and reporter mCherry expression was stable for at least 4 months until the mice were sacrificed. Promoter specific ON bipolar cell sensitization was achieved in mice retina by simple intravitreal viral injection of AAV2 carried genes encoding ambient-light activatable multi-characteristic opsin, vMCO1. Bipolar cells are preserved in the retina even in late-stage degeneration, unlike photoreceptors, thus, making it a rational choice for target cell type. Being close to the photoreceptors, activation of ON bipolar cells preserves as much as possible the visual processing as compared to RGCs. The relatively large number of excitable Bipolar cells in retina is expected to provide higher spatial resolution of regained vision upon vMCO1 treatment, which is yet to be determined in clinical study. Further, unlike RGCs, the bipolar cells do not have lateral extending processes, providing focal activation.

The behavioral improvement of vMCO1 treated mice at ambient light level (~1$\mu W/mm^2$) established its enhanced photo-transduction capabilities. The efficient expression of intravitreally injected viral vector, combined with high photosensitivity of expressed MCO1 mitigates the hitherto faced challenges in optogenetics vision restoration like the use of high intensity light source and or active stimulation device. Use of vertebrate rhodopsin presents an important avenue for use as optogenetic tools for treatment of retinal disorders with photoreceptor degeneration (42). However, vertebrate rhodopsin, used ectopically to control G-coupled signaling in cultured cells, has greater rundown with repeated stimulation and deactivates slowly upon switching off the light stimulation(43). Therefore, use of such rhodopsin may not support patterned vision with eye movement and moving objects. In contrast, restoration of high-sensitivity vision with a fast cone opsin was recently

demonstrated in mice model of retinal degeneration(43). Berry *et. al.* was able to achieve behavioral improvement at white light intensity of 100 μWcm^{-2} in non-dark adapted MW cone opsin-treated animals, which is same as the intensity (1 μW/mm^2) at which significant behavioral improvement was observed in vMCO1 injected mice evaluated via water-maze and optomotor assays, reported here. However, important distinctions can be made between the characteristic of the MW-cone opsin and MCO1. First, though MW-cone opsin is faster than rhodopsin, the off-response time of MW-cone opsin is >10 sec, which is three orders of magnitude higher as compared to the MCO1, which has fast off-response[24] time of ~10 ms (Fig. 1). It is important to note that microbial opsins such as MCO1 have almost 100% photocycle while vertebrate opsins including MW-cone opsin lacks repeatability over multiple stimulations and are inherently limited by bleaching. Another key difference is in the spectral sensitivity. While MW-cone opsin has narrower response, MCO1 has broad spectral response[24] that will allow vision restoration at multiple color environments ranging from blue to red spectrum. Further, optogenetic sensitization of bipolar cells, as reported here, has significant advantages over retinal ganglion cells (RGCs) (43), which are less abundant in the retina. In addition, since bipolar cells are immediately downstream of photoreceptors in visual signaling, photosensitizing bipolar cells are expected to preserve increased visual processing and the signal amplification may also benefit signal quality, particularly at lower light levels.

No detectable changes in ocular structures in the vMCO1 treated *rd10* mice were observed in SD-OCT measurements. Furthermore, no significant increase in immune response was found in the blood serum (studied by ELISA), and retina (immunofluorescence), after vMCO1 injection and transgene expression. In addition, non-detectable vector in non-targeted organs of vMCO1 treated mice make it a safe candidate for clinical studies. Homogeneous expression of vMCO1 opsin was found across the retina in case of intravitreal injection, which is difficult to achieve with the use of sub-retinal injections. Intravitreal injection is used in routine ophthalmic practice, however, in case of limited penetration of AAV through the inner limiting membrane, it may be desirable to carry out sub-retinal injections. Furthermore, in case of geographic atrophies in retina (as in dry-AMD), photosensitization of targeted bipolar cells in degenerated areas can be achieved by local sub-retinal injections. vMCO1 based re-sensitization of a degenerated retina, will allow treatment in patients with retinal dystrophy by intra-ocular injection without the need of any active stimulation device. It must be noted that, while animals with other ocular gene therapy are seeing benefit > 8 yrs, impermanent MCO1 expression may be advantageous as it allows for a 2nd injection if better treatment is available.

Conclusions

Ambient light sensitive MCO1 opens up a new vista for optogenetics based treatment for a wide range of retinal disorders. Ambient light evoked ON bipolar cell driven photocurrent is found to be sufficient to enable activation of the visual circuitry in degenerated mice as reflected in the improved locomotory behavior in case of vMCO1 treated *rd10* mice. We found robust expression of MCO1 opsin in ON bipolar cells by intravitreal injection of vMCO1. This retention of expression translated into maintained behavioral efficacy in the longitudinal measurements. Furthermore, the absence of inflammatory cells in the retina,

non-detectable vector in non-targeted organs, no increase in pro-anti-inflammatory cytokines in plasma or vitreous humor and no increase in the level of neutralizing antibody after vMCO1 injection established safe vMCO1 delivery and reliable transgene integration into retina. Based on the results, we envision that the ambient light sensitive MCO1 based optogenetic stimulation of retina will pave the way for minimally invasive, high resolution, and active stimulation-free treatment of retinal degenerative diseases.

Materials and Methods

Ethics statement

All experimental procedures were conducted according to the Nanoscope Technologies' Institutional Animal Care and Use Committee approved protocol and standard operating procedures (SOPs).

Synthesis and theoretical modeling of vMCO1

The MCO1 gene(44) was synthesized using a DNA synthesizer and the sequence was verified. Synthesized plasmid (MCO1) was cloned into pAAV MCS vector via its BamH1 and Sal1 sites. DNA gel electrophoresis was carried out to verify the size and purity of MCO1 gene (digested by restriction enzymes BamH I and Sal I with restriction fragments). AAV2 physical titers were obtained by quantitative PCR using primers designed to selectively bind AAV inverted terminal repeats. Purification of vMCO1 was carried out by Benzonase-treatment to reduce the size of Host Cell DNA (HCD) and Host Cell Protein (HCP) removal. An SDS PAGE was used to verify the purity of the virus. Highly recognized web-based protocol, "RaptorX" was utilized to develop a theoretical modeling of MCO1.

Mouse preparation

Retinal degenerated mice (B6.CXB1-$Pde6b^{rd10}$/J) and wild type (C57BL/6J) were obtained from Jackson laboratory and bred in the animal facilities of the Nanoscope Technologies. The sample size for behavioral assays was based on the preliminary exploratory study and considering at least 80% power and alpha=0.05. The mice were maintained on a 12:12 light cycle. The average illumination levels in the room was ~200 lux during day though the light reaching the mice inside the cage (mounted in a rack) is expected to be lower. The mice were treated humanely in strict compliance with IACUC on the use of animals in research. The dosing investigator was not blinded, however, the outcome (behavior, imaging, QPCR, etc) accessors and other investigators were blinded in the study.

Preparation of retina explants and transfection

Adult (8 weeks old) *rd10* mice were treated humanely in strict compliance with IACUC on the use of animals in research. Eyes were removed from the euthanized mice. The retinas were removed and cut into pieces of explants using a tissue chopper. The explants were then placed into sterile 35-mm Petri dishes previously coated with 0.5 mg/dish poly-D-lysine (Sigma). The explants were oriented with the ganglion cell side toward the poly-D-lysine and incubated at 37 °C in a 5% CO_2 humidified atmosphere in PNGM™ Primary Neuron Growth Medium (Lonza). Once the retina was attached (after 24-36 hours), the transfection of MCO1 plasmids was carried by lipofection. Briefly, 2 μg of plasmid was mixed with

200 μl of a transfection buffer, followed by 4 μl of transfection reagent, and incubated for 15 mins. The mixture was added dropwise into the retinal culture media in a 35 mm petri dish and transfection was confirmed after 48-72 hrs of transfection under microscope by visualizing the mCherry fluorescence.

Intravitreal injection of vMCO1 to rd10 mouse eye

Aseptic technique was used for all surgical procedures and surgical tools were sterilized with an autoclave. The *rd10* mice (>12 weeks old) was anesthetized and local anesthesia (proparacaine) was applied onto the eyes of the animals. The vMCO1 (1 μl) solution was injected by a sterilized 29-gauge needle of a Hamilton micro-syringe, inserted through the sclera into the vitreous cavity (intravitreal injection). The vMCO1 solution was injected into both of the eyes. In the case of control, 1 μl rAAV2 empty backbone (vehicle) for water maze behavior or PBS (for evaluating expression) was injected into the eyes intravitreally by a sterilized 29-gauge needle. The cornea was kept moist with a balanced salt solution during the surgical procedure.

Quantification of MCO1 expression in rd10 mouse retina

In-vivo intravitreal injection of vMCO1 in *rd10* mouse retina was carried out for three different final doses of vMCO1: 1.0×10^{10}, 1.0×10^{9} and 1.0×10^{8} vg/eye. At different time points after vMCO1 intravitreal injection, the mice in each group (N=5) were euthanized and the eye cups were fixed for 30 min in 4% PFA and were stored in PBS. Low magnification (4X) confocal fluorescence microscopy was utilized to visualize the mCherry reporter expression in red detection channel, and intrinsic average fluorescence intensity (area normalized) analysis of multiple (N=5) regions in each image was carried out using ImageJ to quantify the expression level at different time points after intravitreal injection at different doses of vMCO1.

Optogenetic stimulation

A single mode optical fiber coupled to a supercontinuum laser source (SuperK Compact, NKT Photonics) delivered light to the sample via fiber optic cable (SuperK FD-2), which transmits light in the visible spectrum for *in-vitro* optogenetic stimulation. A power meter (Newport) was used to measure the light intensity at the sample plane. The light pulse width was controlled electronically, synchronized with the electrophysiology recording system (Molecular Devices).

Patch-clamp recording

Inward photocurrents in MCO1 transfected retinal cells were recorded using patch clamp system consisting of inverted Nikon fluorescence microscope, a high-resolution, low-noise digitizer and an amplifier system (Axon Multiclamp 700B, Molecular Devices). Micropipettes were pulled using a two-stage pipette puller (PC-10, Narshige) to attain resistance of 3 to 5 MΩ when filled with intra-cellular solution containing (in mM) 130 K-Gluoconate, 7 KCl, 2 NaCl, 1 $MgCl_2$, 0.4 EGTA, 10 HEPES, 2 ATP-Mg, 0.3 GTP-Tris and 20 sucrose. The extracellular solution contained (in mM): 150 NaCl, 10 Glucose, 5 KCl, 2 $CaCl_2$, 1 $MgCl_2$ was buffered with 10 mM HEPES (pH 7.3). Photocurrents were

measured while holding cells in voltage clamp at –70 mV. The electrophysiological signals from the amplifier were digitized using Digidata 1440 (Molecular devices), interfaced with patch-clamp software (pClamp, Molecular Devices). The light pulse was synchronized with the electrophysiology recording system, controlled by Axon Instruments Digidata system. pClamp 10 software was used for data analysis.

Visually guided water maze behavioral assessment

Rd10 mice with retinal degeneration were used following inclusion criteria: age > 8 weeks (N=5/group). Both vMCO1 injected and vehicle (AAV2) injected mice groups were trained for 1 week before establishment of baseline (i.e. 2 weeks before injection) behavioral scores. Before vMCO1 injection, the baseline of visually guided behavior in radial water maze was established. Briefly, mice were placed into the center of the maze and a platform was placed just below the water's surface at the end of one of the arms. The mice rapidly learned to determine the location of the platform by utilizing visual cues (LEDs emitting light with visible spectrum). The platform (in one of the arms) provided a reward to them where they can rest instead of having to swim. The time to reach platform was quantified in presence of visual-guidance cue. Data (video) recording was stopped once the mice found the platform, or after 60 seconds of placing the mice in water to prevent fatigue induced drowning. After vMCO1 injection, mice were tested in the radial arm water maze to determine behavioral restoration of vision in *rd10* mice with vMCO1-sensitized retinal cells. For each mouse, 3 trials were conducted in each location (i.e., center, side and arm of the water maze). The selection of the dropping site (center, side, arm), was random for each mouse and each trial. The pre-established exclusion criterion consists of mice that do not swim (and floats).

Optomotor response after vMCO1 treatment

Since the measurement of the opto-motor response is commonly used to determine thresholds of the visual system in animals (36, 37), we utilized this tool for evaluating improvement in visual performance of retinal degenerated mice with vMCO1 sensitized retinas. Briefly, mice were placed on a platform (in the center of a drum) surrounded by rotating vertical stripes, generated by LCD display screens (1 $\mu W/mm^2$) attached to a laptop. The average optomotor response (head movement at different rotational speed of vertical stripes) was measured at 2-time points (before and after 8 weeks of vMCO1 injection). We evaluated functional recovery of vision via head tracking response. The basic principle of this analysis is: whenever a moving pattern is presented to a light sensing animal, the animal will move its head as a transient corrective measure to maintain stable vision. The advantage of this method is that it does not require any previous training of the animal.

Collection of blood at different time points after injection of vMCO1 in mice

After anesthetization, blood (~0.2 ml) is drawn from facial vein (using sterile animal lancet) 1 week before intravitreal injection. After vMCO1 injection, blood was drawn at different time points for analysis. After the completion of the study period (6 months), the mouse was euthanized. For collecting the blood from the facial vein of the mice, the hairless freckle on the side of the jaw was located and pricked with a lancet.

Immunostaining

The vMCO1-injected eyes were collected from the mice after 8 weeks of intravitreal injection. Harvested eyes were fixed in 4% paraformaldehyde for 30 min and were stored in PBS for cryo-sectioning. S-Arrestin (1:1000), PKCα (1:200), mCherry (1:500), GFAP (1:500) and CD45 (1:500) primary antibodies were obtained from Thermo Fisher Scientific and Iba1 (1:250) primary antibody was obtained from Santa Cruz Biotechnology. The secondary (DyLight 488, Alexa Fluor 568, 1: 500 dilution) antibodies were obtained from Thermo Fisher Scientific. Retina slices were made horizontally at the inner layer of the retina using a cryostat. Blocking solution (4% goat serum in washing solution) was added into the tissue samples on glass slide for 1 hour at room temperature. One hour later, blocking solution was removed and primary antibody was added and incubated at 4°C. The next day, the primary antibody was removed, and samples were washed 3 times (each time/10 minutes) with washing solution (0.5% triton in 1xPBS). After washing, the secondary antibody was added and kept in a dark enclosure for 1 hour at room temperature. One hour later, the secondary antibody was removed, and the samples were washed 3 times (10 min) with 0.5% triton in 1xPBS. After washing, DAPI solution was added for 15 minutes at room temperature. 15 minutes later, the DAPI solution was removed and the samples were washed twice (5 min for each washing) with 1xPBS. After washing, one drop of mounting medium was applied, and the cover glass was placed. Immunostained tissue samples were dried under dark conditions for at least 2 hours prior to confocal imaging. Images were taken by confocal microscope (Olympus Fluoview FV1000) using the laser with excitation lines at 405 nm (for DAPI), 488 nm (for DyLight 488) and 543 nm (for intrinsic mCherry and Alexa Fluor 568). Image processing was performed using ImageJ software.

Tissue collection for bio-distribution analysis

Each group (transfected with vMCO1 of different doses and different sacrifice time points) contained 5 *rd10* mice. After euthanizing the mice, tissues of different organs (i.e., Blood, Brain, Eyes, Heart, Kidney, Liver, and Spleen) were collected at different time points after vMCO1 injection. The tissues were snap-frozen in the cryo-vials and stored at −80 °C for further analysis. The left-over eye-tissues (after slicing of posterior part, i.e. retina) were used for biodistribution analysis using QPCR.

DNA extraction and qPCR

Genomic DNA was extracted from tissue samples using the IBI Scientific Genomic DNA Mini Kit (Cat# IB47222, Lot# FB11709) according to the manufacturer's protocol and diluted to a concentration of 10 ng/µL. Primers for the QPCR assay were designed using Primer 3(45). Sequences for the primers were as follows: Forward: 5'-AAACTGAACATTGGCGGCAC-3'; Reverse: 5'-CATTCCTCCACAGCCCATGT-3'. Melting curve analysis was performed to ensure single-product amplification for the primer pair. Real time PCR was performed on the ABI 7900HT Fast Real Time PCR System (Applied Biosystems) using assays specific (195 bp fragment) for gene of interest. Each reaction well contained 5µL of PowerUp SYBR® Green PCR Master Mix (Applied Biosystems, Cat# A25742, Lot# 1704034), 20 ng of DNA and 250 nM each of forward

and reverse amplification primers in a reaction volume of 10 μL. Cycling conditions were as follows: 95 °C for 10 minutes for polymerase activation, followed by 40 cycles of 95 °C for 15 seconds and 60 °C for 1 minute. Data analysis was performed using Sequence Detection System software from Applied Biosystems, version 2.4. The experimental samples' Ct (cycle threshold) values were calibrated against a standard curve of pAAV-MCS containing the specific (195 bp fragment) gene sequence. The samples were analyzed in triplicate for copy number by the Absolute Quantification method (46).

Immunosorbent assay (ELISA) of serum derived from vMCO1 injected rd10 mice

ELISA Studies on kinetics of immunotoxicity were conducted using mouse Picokine ELISA (BosterBio) based quantification of different pro and anti-inflammatory cytokines (IL-6, IL-10) in plasma of vMCO1-treated animals at different time points and vitreous humor after sacrificing the animal. The ELISA manufacturer's protocol was followed for analysis of serum and vitreous humor derived from mice injected with vMCO1 as well as control (non-injected) and microplate reader (BIOTEK) was used for quantification.

Neutralizing Antibody assay in serum from vMCO1 injected rd10 mice

The neutralizing antibody assay was performed to evaluate any pre-existing antibody for vMCO1 and to monitor the changes in the neutralizing antibody level following vMCO1 injection. The 96 wells plate was coated with 100μl of positive standard (vMCO1) and blocked with 2% BSA (100μl) in PBS at Room temperature (RT) for 1 hour. The plate was washed twice with 100μl of 2% sucrose in PBS. For generating standard curve, serial dilution of stock antibody solution was carried out and added to pre-assigned wells in the plate. The mice serum samples (from injected and control group) were diluted at 1:40 with PBS containing 0.1% BSA to each well (100 μL/well). The samples in the plate were incubated for 1 hour at RT, washed two times with PBS containing 0.05% Tween 20. A solution containing 1X horseradish peroxidase-conjugated anti-human immunoglobulin G (HRP-IgG) was added to each well (100 μL/well). The sample-plate was incubated for 1 hour at RT and washed two times with PBS containing 0.05% Tween 20. Addition of 100 μL 3,3′,5,5′-tetramethylbenzidine/urea hydrogen peroxide and incubation for 30 min at RT led to development of blue coloration. The color development was stopped by adding 0.5% sulfuric acid (100 μL/well) without removing the substrate from the wells. The optical density (OD) of the sample (color: yellow) at 450/640 nm was measured using a microplate reader (BIOTEK).

Optical Coherence Tomographic (OCT) imaging

The mice were anesthetized with a mixture of ketamine (65 mg/kg), xylazine (7.5 mg/kg), and acepromazine (0.5 mg/kg) and mounted on a maneuverable imaging platform. 1~2 drops of 1% tropicamide was topically applied to eyes for pupil dilation. The cornea was kept moist with a balanced salt solution during the measurement period. Spectral Domain-OCT (SD-OCT) imaging(47-49) was performed before and within 1 week of vMCO1 injection. Retinal thickness measurements were made at different locations of the retina before and after vMCO1 injection.

Statistical Analysis

GraphPad Prism was used to analyze data. The data were plotted as Mean ± S. D. For data with multiple variables such as dose and time response (water-maze assay), one-way ANOVA with Tukey post hoc analysis was carried out. Otherwise, statistically significant difference analyses were carried out by t-test. $p < 0.05$ was considered statistically significant.

Supplementary Material

Refer to Web version on PubMed Central for supplementary material.

Acknowledgements

References

1. Takeda A, Baffi JZ, Kleinman ME, Cho WG, Nozaki M, Yamada K, et al. CCR3 is a target for age-related macular degeneration diagnosis and therapy. Nature. 2009;460(7252):225–U87. [PubMed: 19525930]

2. Schuchard RA, Naseer S, de Castro K. Characteristics of AMD patients with low vision receiving visual rehabilitation. J Rehabil Res Dev. 1999;36(4):294–302. [PubMed: 10678452]

3. Yang ZL, Camp NJ, Sun H, Tong ZZ, Gibbs D, Cameron DJ, et al. A variant of the HTRA1 gene increases susceptibility to age-related macular degeneration. Science. 2006;314(5801):992–3. [PubMed: 17053109]

4. Haines JL, Hauser MA, Schmidt S, Scott WK, Olson LM, Gallins P, et al. Complement factor H variant increases the risk of age-related macular degeneration. Science. 2005;308(5720):419–21. [PubMed: 15761120]

5. Humayun M, Dorn J, da Cruz L. Interim results from the international trial of Second Sight's visual prosthesis. Ophthalmology. 2012;119:779–88. [PubMed: 22244176]

6. Pan ZH, Lu Q, Bi A, Dizhoor AM, Abrams GW. Optogenetic Approaches to Restoring Vision. Annu Rev Vis Sci. 2015;1:185–210. [PubMed: 28532375]

7. Sahel JA, Roska B. Gene therapy for blindness. Annu Rev Neurosci. 2013;36:467–88. [PubMed: 23724995]

8. Zrenner E Will retinal implants restore vision? Science. 2002;295(5557):1022–5. [PubMed: 11834821]

9. Humayun MS. Intraocular retinal prosthesis. Trans Am Ophthalmol Soc. 2001;99:271–300. [PubMed: 11797315]

10. Doyle SL, Campbell M, Ozaki E, Salomon RG, Mori A, Kenna PF, et al. NLRP3 has a protective role in age-related macular degeneration through the induction of IL-18 by drusen components. Nat Med. 2012;18(5):791–8. [PubMed: 22484808]

11. Humayun MS, Weiland JD, Fujii GY, Greenberg R, Williamson R, Little J, et al. Visual perception in a blind subject with a chronic microelectronic retinal prosthesis. Vision research. 2003;43(24):2573–81. [PubMed: 13129543]

12. Margalit E, Maia M, Weiland JD, Greenberg RJ, Fujii GY, Torres G, et al. Retinal prosthesis for the blind. Survey of ophthalmology. 2002;47(4):335–56. [PubMed: 12161210]

13. Zrenner E Fighting blindness with microelectronics. Sci Transl Med. 2013;5(210):210ps16.

14. Hetling JR, Baig-Silva MS. Neural prostheses for vision: designing a functional interface with retinal neurons. Neurol Res. 2004;26(1):21–34. [PubMed: 14977054]

15. Palanker D, Vankov A, Huie P, Baccus S. Design of a high-resolution optoelectronic retinal prosthesis. J Neural Eng. 2005;2(1):S105–20. [PubMed: 15876646]

16. Horsager A, Greenwald SH, Weiland JD, Humayun MS, Greenberg RJ, McMahon MJ, et al. Predicting visual sensitivity in retinal prosthesis patients. Invest Ophthalmol Vis Sci. 2009;50(4):1483–91. [PubMed: 19098313]

17. de Balthasar C, Patel S, Roy A, Freda R, Greenwald S, Horsager A, et al. Factors affecting perceptual thresholds in epiretinal prostheses. Invest Ophthalmol Vis Sci. 2008;49(6):2303–14. [PubMed: 18515576]

18. Zrenner E, Bartz-Schmidt KU, Benav H, Besch D, Bruckmann A, Gabel VP, et al. Subretinal electronic chips allow blind patients to read letters and combine them to words. Proc Biol Sci. 2011;278(1711):1489–97. [PubMed: 21047851]

19. Chow AY, Pardue MT, Perlman JI, Ball SL, Chow VY, Hetling JR, et al. Subretinal implantation of semiconductor-based photodiodes: durability of novel implant designs. J Rehabilit Res Develop. 2002;39(3):313–21.

20. Zrenner E Will Retinal Implants Restore Vision? Science. 2002;295(5557):1022–5. [PubMed: 11834821]

21. Banghart M, Borges K, Isacoff E, Trauner D, Kramer RH. Light-activated ion channels for remote control of neuronal firing. Nature neuroscience. 2004;7(12):1381. [PubMed: 15558062]

22. Caporale N, Kolstad KD, Lee T, Tochitsky I, Dalkara D, Trauner D, et al. LiGluR restores visual responses in rodent models of inherited blindness. Molecular therapy. 2011;19(7):1212–9. [PubMed: 21610698]

23. Polosukhina A, Litt J, Tochitsky I, Nemargut J, Sychev Y, De Kouchkovsky I, et al. Photochemical restoration of visual responses in blind mice. Neuron. 2012;75(2):271–82. [PubMed: 22841312]

24. Wright W, Gajjeraman S, Batabyal S, Pradhan S, Bhattacharya S, Mahapatra V, et al. Restoring vision in mice with retinal degeneration using multicharacteristic opsin. Neurophotonics. 2017;4(4):041505. [PubMed: 28948190]

25. Batabyal S, Cervenka G, Ha JH, Kim YT, Mohanty S. Broad-Band Activatable White-Opsin. PLoS One. 2015;10(9):e0136958. [PubMed: 26360377]

26. Tochitsky I, Kramer RH. Optopharmacological tools for restoring visual function in degenerative retinal diseases. Curr Opin Neurobiol. 2015;34:74–8. [PubMed: 25706312]

27. Barrett JM, Berlinguer-Palmini R, Degenaar P. Optogenetic approaches to retinal prosthesis. Vis Neurosci. 2014;31(4-5):345–54. [PubMed: 25100257]

28. Marc R, Pfeiffer R, Jones B. Retinal prosthetics, optogenetics, and chemical photoswitches. ACS Chem Neurosci. 2014;5(10):895–901. [PubMed: 25089879]

29. Garg SJ, Federman J. Optogenetics, visual prosthesis and electrostimulation for retinal dystrophies. Curr Opin Ophthalmol. 2013;24(5):407–14. [PubMed: 23799487]

30. Wu C, Ivanova E, Zhang Y, Pan ZH. rAAV-mediated subcellular targeting of optogenetic tools in retinal ganglion cells in vivo. PLoS One. 2013;8(6):e66332. [PubMed: 23799092]

31. Goetz GA, Mandel Y, Manivanh R, Palanker DV, Cizmar T. Holographic display system for restoration of sight to the blind. J Neural Eng. 2013;10(5):056021. [PubMed: 24045579]

32. Macé E, Caplette R, Marre O, Sengupta A, Chaffiol A, Barbe P, et al. Targeting channelrhodopsin-2 to ON-bipolar cells with vitreally administered AAV restores ON and OFF visual responses in blind mice. Mol Ther. 2015;23(1):7–16. [PubMed: 25095892]

33. Busskamp V, Duebel J, Balya D, Fradot M, Viney TJ, Siegert S, et al. Genetic reactivation of cone photoreceptors restores visual responses in retinitis pigmentosa. science. 2010;329(5990):413–7. [PubMed: 20576849]

34. Schiller PH, Sandell JH, Maunsell JH. Functions of the ON and OFF channels of the visual system. Nature. 1986;322(6082):824. [PubMed: 3748169]

35. Hodges H. Maze procedures: the radial-arm and water maze compared. Brain Res Cogn Brain Res. 1996;3(3-4):167–81. [PubMed: 8806020]

36. Prusky GT, Alam NM, Beekman S, Douglas RM. Rapid quantification of adult and developing mouse spatial vision using a virtual optomotor system. Invest Ophthalmol Vis Sci. 2004;45(12):4611–6. [PubMed: 15557474]

37. Douglas RM, Alam NM, Silver BD, McGill TJ, Tschetter WW, Prusky GT. Independent visual threshold measurements in the two eyes of freely moving rats and mice using a virtual-reality optokinetic system. Vis Neurosci. 2005;22(5):677–84. [PubMed: 16332278]

38. Tomita H, Sugano E, Isago H, Hiroi T, Wang Z, Ohta E, et al. Channelrhodopsin-2 gene transduced into retinal ganglion cells restores functional vision in genetically blind rats. Experimental eye research. 2010;90(3):429–36. [PubMed: 20036655]

39. Li S, Huang L. Nonviral gene therapy: promises and challenges. Gene Ther. 2000;7(1):31–4. [PubMed: 10680013]

40. Thomas CE, Ehrhardt A, Kay MA. Progress and problems with the use of viral vectors for gene therapy. Nat Rev Genet. 2003;4(5):346–58. [PubMed: 12728277]

41. Doroudchi MM, Greenberg KP, Liu J, Silka KA, Boyden ES, Lockridge JA, et al. Virally delivered channelrhodopsin-2 safely and effectively restores visual function in multiple mouse models of blindness. Mol Ther. 2011;19(7):1220–9. [PubMed: 21505421]

42. Gaub BM, Berry MH, Visel M, Holt A, Isacoff EY, Flannery JG. Optogenetic retinal gene therapy with the light gated GPCR vertebrate rhodopsin. Retinal Gene Therapy: Springer; 2018. p. 177–89.

43. Berry MH, Holt A, Salari A, Veit J, Visel M, Levitz J, et al. Restoration of high-sensitivity and adapting vision with a cone opsin. Nature communications. 2019;10(1):1–12.

44. Mohanty S, Bhattacharya S, inventors; Nanoscope Technologies LLC, assignee. Optogenetic modulation by multi-characteristic opsins for vision restoration and other applications thereof. Australia patent 2017372351. 2017.

45. Ye J, Coulouris G, Zaretskaya I, Cutcutache I, Rozen S, Madden TL. Primer-BLAST: A tool to design target-specific primers for polymerase chain reaction. BMC Bioinformatics. 2012;13(1):134. [PubMed: 22708584]

46. Brankatschk R, Bodenhausen N, Zeyer J, Burgmann H. Simple absolute quantification method correcting for quantitative PCR efficiency variations for microbial community samples. Appl Environ Microbiol. 2012;78(12):4481–9. [PubMed: 22492459]

47. Liu Y, McDowell CM, Zhang Z, Tebow HE, Wordinger RJ, Clark AF. Monitoring retinal morphologic and functional changes in mice following optic nerve crush. Invest Ophthalmol Vis Sci. 2014;55(6):3766–74. [PubMed: 24854856]

48. Kim BJ, Silverman SM, Liu Y, Wordinger RJ, Pang IH, Clark AF. In vitro and in vivo neuroprotective effects of cJun N-terminal kinase inhibitors on retinal ganglion cells. Mol Neurodegener. 2016;11:30. [PubMed: 27098079]

49. Kim BJ, Sprehe N, Morganti A, Wordinger RJ, Clark AF. The effect of postmortem time on the RNA quality of human ocular tissues. Mol Vis. 2013;19:1290–5. [PubMed: 23805035]

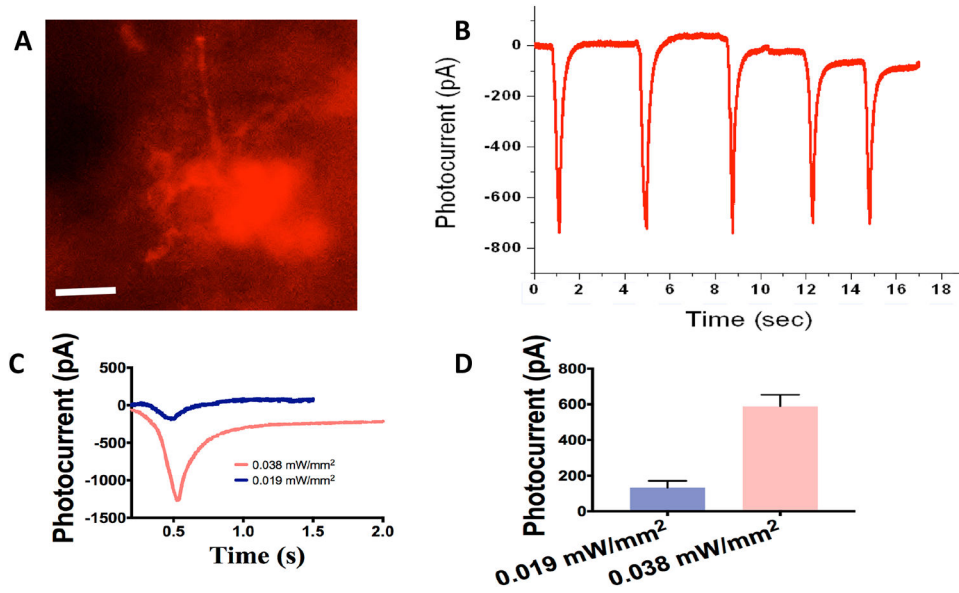Author Manuscript   Author Manuscript   Author Manuscript   Author Manuscript

Fig. 1: Expression of ambient light activatable Multi-Characteristic Opsin (MCO1) in retinal explant of *rd10* mice led to significant photocurrent.

(A) Representative image showing MCO1 expression in the mice (12 weeks old) retinal explants (4 days after transfection by lipofection). Scale bar: 20 μm. (B) Representative inward photocurrent induced by light pulse (100 ms) train at intensity of 0.038 mW/mm^2. (C) Representative profiles of inward photocurrent in retinal cell expressing MCO1 at two different light intensities. (D) Variation of photocurrent as a function of stimulation light intensity. Average ± S.D. N= 3 cells (n= 7-14 sweeps/ intensity).
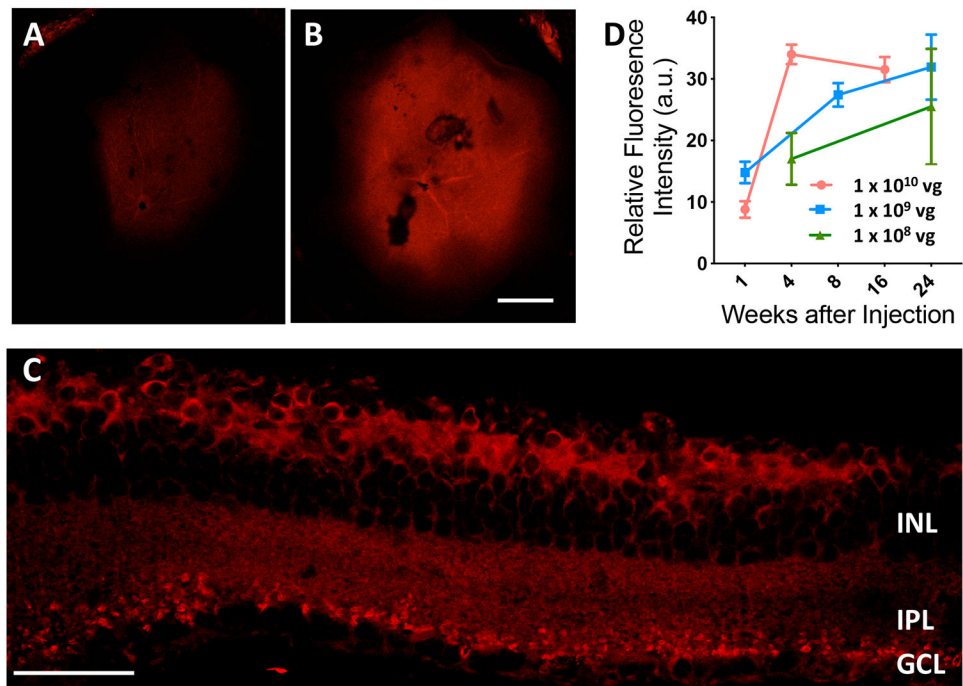
Fig. 2: Kinetics of vMCO1-dose dependent expression in mouse retina.
Representative low magnification (4X) fluorescence confocal image of retina cup after (A)
1 week, (B) 8 weeks after intravitreal injection of vMCO1 (1.0 x 10^{10} vg in eye) into *rd10*
mice (12 weeks old). Scale bar: 200 μm. (C) Confocal mCherry fluorescence image of
cross-section of retina transfected with vMCO1 at dose of 1.0 x 10^{10} vg. Scale bar: 50 μm.
(D) Kinetics of MCO1 expression quantified by means of measured reporter gene (mCherry)
expression in *rd10* mice retina at three different doses of vMCO1. Average ± SD. N=4.
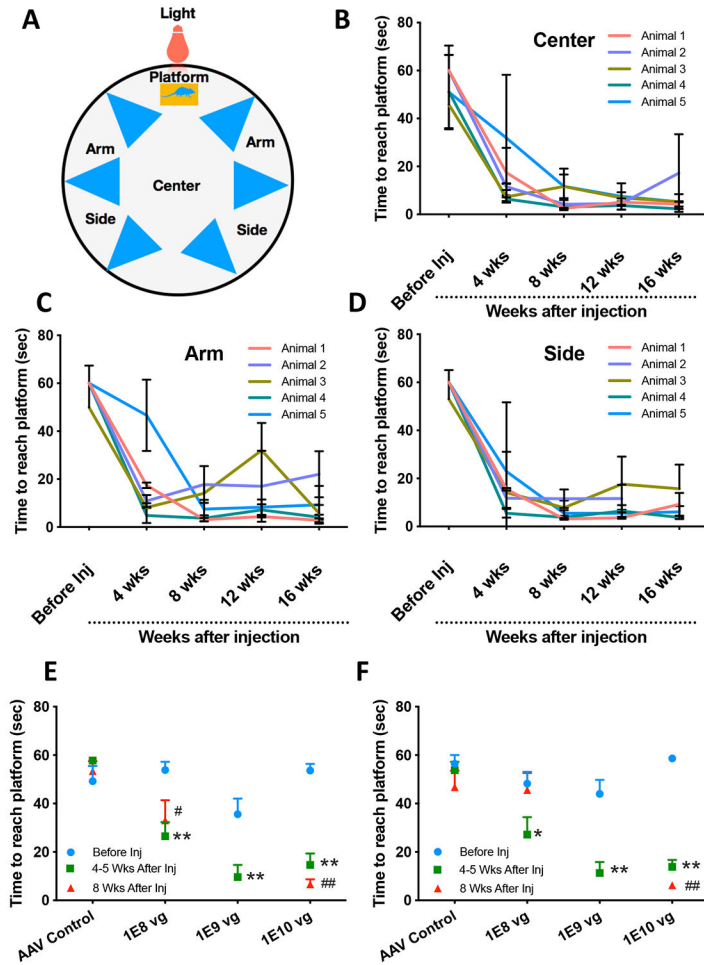
Fig. 3: Intravitreal injection of vMCO1 in *rd10* mice led to ambient-light guided locomotion in a longitudinal manner.

(A) Schematic of water maze set up representing different locations and platform. (B) Time to reach platform (latency) by the mice (injected at age of 12 weeks) from center of the maze (light intensity: 7 μW/mm^2) as a function of 16-week post-injection period. (C) Latency to reach platform by the mice from near arm of the maze (light intensity: 1 μW/mm^2) as a function of 16-week post-injection period. (D) Time to reach platform from the side of the maze (light intensity: 2 μW/mm^2) as a function of 16-week post-injection period. Intravitreal vMCO1 dose (1.0x10^{10}, 1.0x10^9 and 1.0x10^8 vg) response of mice along with AAV2 vehicle control measured by water maze latency score for center (E) and side (F) at baseline, 4-5 weeks and 8 weeks after injection. N=5; Average $\pm$ S.D., *p<0.05 between Before and 4-5 weeks, **p<0.01 between Before and 4-5 weeks, #p<0.05 between Before and 8 weeks, ##p<0.01 between Before and 8 weeks, No statistical difference between 4 weeks and 8 weeks all dose.
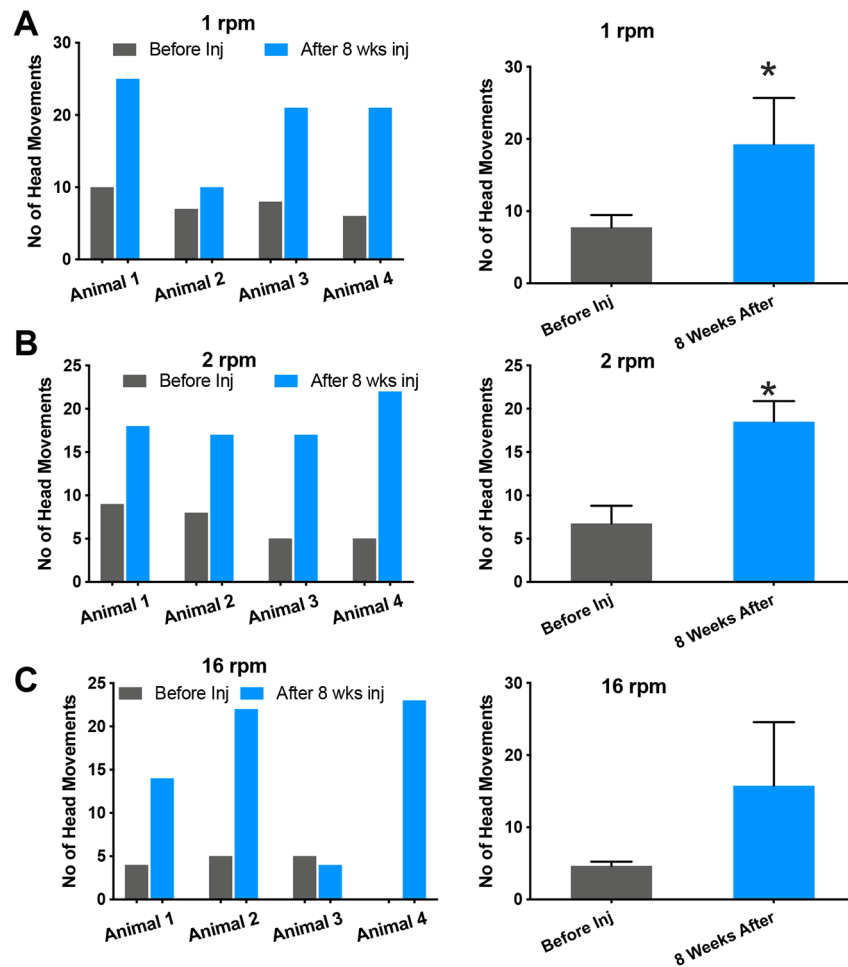
Fig. 4: Improvement of optomotor response in vMCO1 treated *rd10* mice at ambient light level. Quantitative comparison of number of head movement at different speed of rotation of the vertical stripes: (A) 1 rpm, and (B) 2 rpm, between before and 8 weeks after intravitreal injection of vMCO1 (1.0×10^{10} vg) in 12 weeks old mice. vMCO1 treated *rd10* mice shows improved optomotor response as reflected in the increase head movement after vMCO1 injection. Average + SD. N=4. *p< 0.05. The average light intensity at the center of the chamber was 1 μW/mm^2.
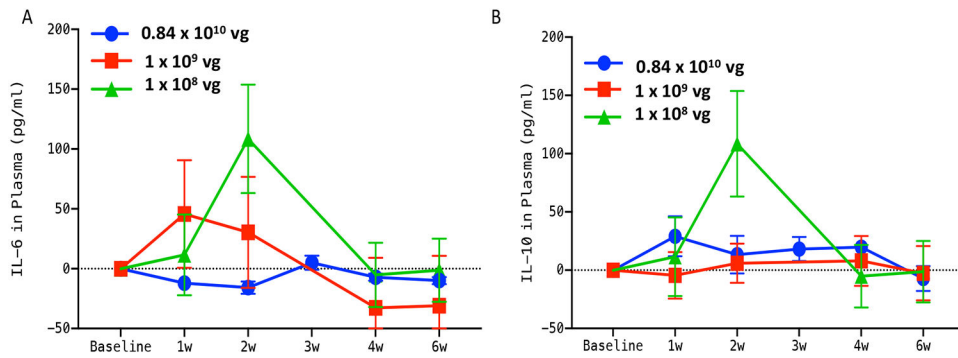
Fig. 5: No detectable increase in inflammatory response in plasma of *rd10* mice after vMCO1 injection.

(A) Quantitative comparison of change in IL-6 (pro-inflammatory marker) from baseline in plasma between group-1 (1.0 x 10^8 vg in eye), group-2 (1.0 x 10^9 vg) and group-3 (0.84 x 10^{10} vg) *rd10* mice at 1,2, 3, 4, and 6 weeks after vMCO1 injection at the age of 12 weeks. (B) Quantitative comparison of change in IL-10 (anti-inflammatory marker) from baseline between the groups. Average ± SD. N=5 for 1.0 x 10^8 vg and 1.0 x 10^9 vg and N=3 for 0.84 x 10^{10} vg.
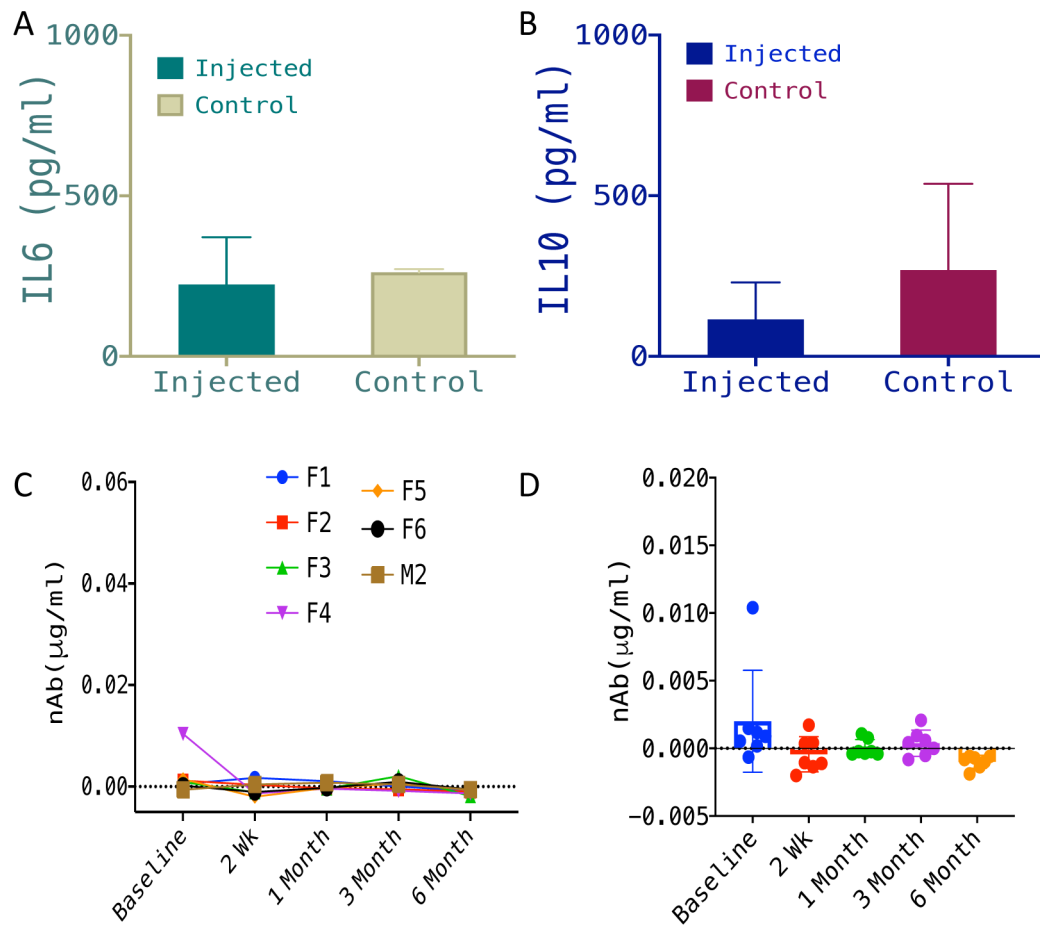
Fig. 6: No detectable inflammatory response in vitreous humor or immune response in plasma of vMCO1 injected mice.

Quantitative comparison of IL-6 (pro-inflammatory marker) (A) and IL-10 (anti-inflammatory marker) (B) in vitreous humor of *rd10* mice injected with vMCO1 (1.0 x 10^9 vg in eye) and non-injected control, 6 months after vMCO1 injection (at the age of 12 weeks). Average ± SD. N=7. (C) Longitudinal monitoring of neutralizing Antibody (nAb) level in serum of *rd10* mice injected with vMCO1 (1.0 x 10^9 vg in eye) before and after injection (F: Female; M: Male) at 12 weeks of age. (D) Scatter plot showing the mean and variation of measured neutralizing antibody concentration in serum of vMCO-010 injected *rd10* mice at each time point. N=7.
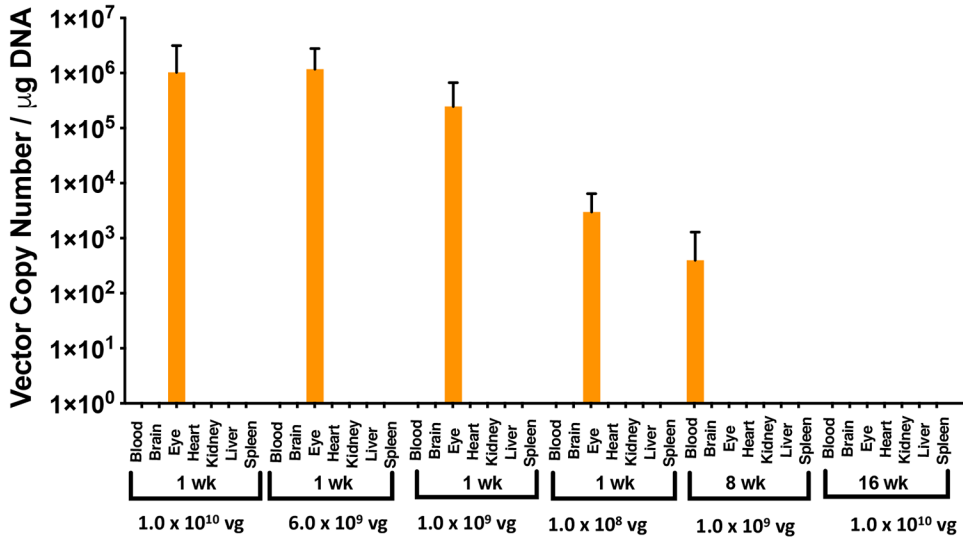
Fig. 7: Bio-distribution show non-detectable levels of the vector in non-targeted organs of intravitreally-injected *rd10* mice.

Distribution of the AAV2 vector was quantified by qPCR in 7 different tissues, including the injected eyes of the mice (age: 12 weeks), at different time points and vMCO1 doses (1.0×10^{10}, 6.0×10^9, 1.0×10^9 and 1.0×10^8 vg/eye). qPCR analysis showed the presence of AAV2 in treated eyes after first week of injection. Negligible quantities of AAV2 vector copies were identified in some tissues (not visible in the graph). Average ± SD. N=5.
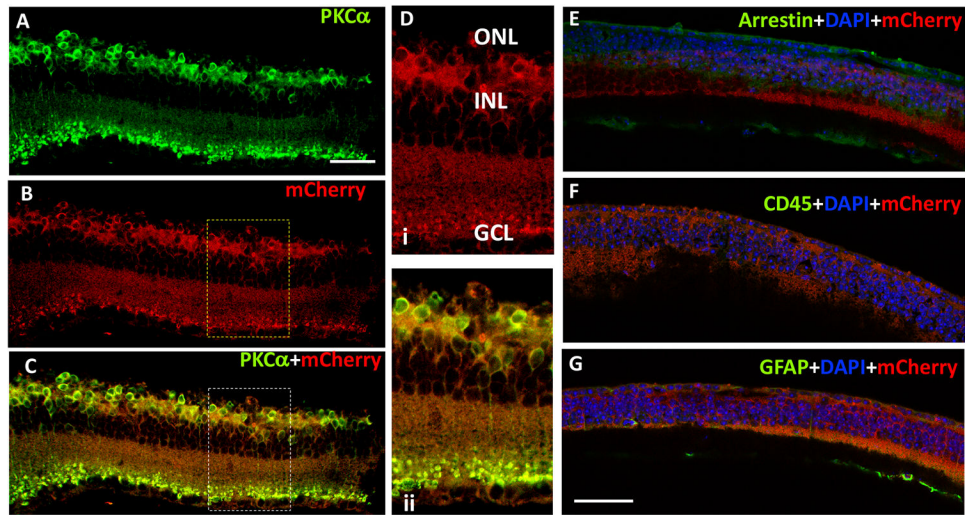
Fig. 8: Intravitreal injection of vMCO1 led to ON-bipolar specific expression in *rd10* mice retina without causing inflammatory-response.

The cryo-sectioned retinal slices were immunostained using primary antibodies with different dilution (PKCα- 1:200; mCherry-1: 500; Arrestin-1: 1000; GFAP-1: 500; CD45-1: 500) and DyLight 488 (1: 500 dilution) as a secondary antibody. PKCα stain (green, A) showing bipolar cells expressing MCO1 (visualized by intrinsic mCherry expression 16 weeks after injection of vMCO-1 (1.0 x 10^{10} vg) in 12 weeks old *rd10* mice, B). High levels of colocalization with virally expressed MCO1 in bipolar cells, evident in (C). (D) Representative high-resolution zoomed picture showing membrane expression of MCO1 in bipolar cells and overlay picture of mCherry and PKCα confirming co-localization. (E) Absence of S-arrestin (green) confirms complete loss of photoreceptors. (F) Absence of CD45 (green) marker suggests no detectable immune cells after vMCO1 injection. (G) GFAP (green) observed as reported in photoreceptor degenerated retina. Scale: 50 μm.
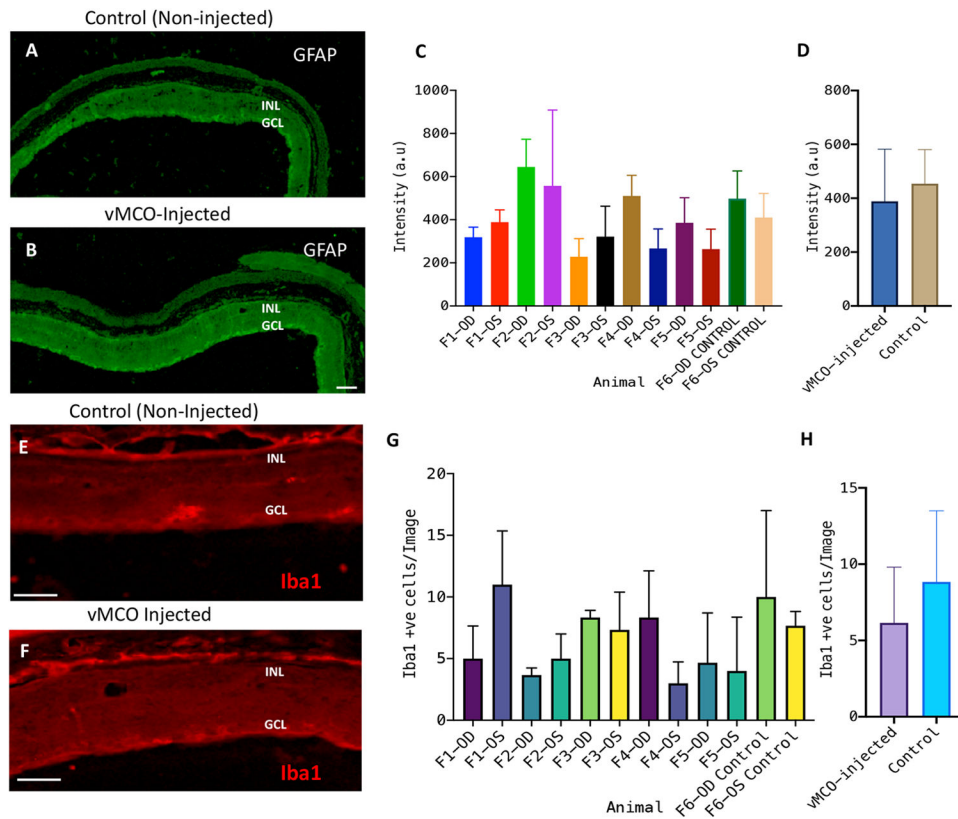
Fig. 9: Intravitreal injection of vMCO1 did not cause cellular inflammatory response in retina of *rd10* mice.

The cryo-sectioned retinal slices were immunostained using primary antibodies (Iba1 for microglia and GFAP for glial cells) and secondary antibodies (DyLight 488 for GFAP and Alexa Fluor 568 for Iba1). Representative confocal fluorescence microscope image of GFAP-stained retina of (A) non-injected control and (B) vMCO1 (3.5×10^9 vg/eye) injected mice eyes 6 months after bilateral injection. Scale: 50 μm. (C) Quantification of fluorescence intensity of GFAP-labeled retina for individual mice (F1-F5) showing inter-animal variability along with the non-injected negative control. Average ± SD. N=3 retina slices/mouse. (D) No statistically significant difference in fluorescence intensity of GFAP-labeled retina between the vMCO1-injected group and negative control. Representative confocal fluorescence microscope image of Iba1-stained retina of (E) non-injected control and (F) vMCO1(3.5×10^9 vg/eye) injected mice eyes 6 months after bilateral injection. Scale: 50 μm. (G) Quantification of Iba1+ve cells for individual mice (F1-F5) showing inter-animal variability along with the non-injected negative control. Average ± SD. N=3 retina slices/mouse. (H) No statistically significant difference in Iba1+ cells between the vMCO1-injected group and negative control.